Fermilab FERMILAB-Pub-00/133-E CDF July 2000

Measurement of $d\sigma/dy$ for High Mass Drell-Yan e^+e^- Pairs from $p\bar{p}$ Collisions at $\sqrt{s} = 1.8$ TeV

T. Affolder,[21] H. Akimoto,[43] A. Akopian,[36] M. G. Albrow,[10] P. Amaral,[7] S. R. Amendolia,[32] D. Amidei,[24] K. Anikeev,[22] J. Antos,[1] G. Apollinari,[10] T. Arisawa,[43] T. Asakawa,[41] W. Ashmanskas,[7] M. Atac,[10] F. Azfar,[29] P. Azzi-Bacchetta,[30] N. Bacchetta,[30] M. W. Bailey,[26] S. Bailey,[14] P. de Barbaro,[35] A. Barbaro-Galtieri,[21] V. E. Barnes,[34] B. A. Barnett,[17] M. Barone,[12] G. Bauer,[22] F. Bedeschi,[32] S. Belforte,[40] G. Bellettini,[32] J. Bellinger,[44] D. Benjamin,[9] J. Bensinger,[4] A. Beretvas,[10] J. P. Berge,[10] J. Berryhill,[7] B. Bevensee,[31] A. Bhatti,[36] M. Binkley,[10] D. Bisello,[30] R. E. Blair,[2] C. Blocker,[4] K. Bloom,[24] B. Blumenfeld,[17] S. R. Blusk,[35] A. Bocci,[32] A. Bodek,[35] W. Bokhari,[31] G. Bolla,[34] Y. Bonushkin,[5] D. Bortoletto,[34] J. Boudreau,[33] A. Brandl,[26] S. van den Brink,[17] C. Bromberg,[25] M. Brozovic,[9] N. Bruner,[26] E. Buckley-Geer,[10] J. Budagov,[8] H. S. Budd,[35] K. Burkett,[14] G. Busetto,[30] A. Byon-Wagner,[10] K. L. Byrum,[2] P. Calafiura,[21] M. Campbell,[24] W. Carithers,[21] J. Carlson,[24] D. Carlsmith,[44] J. Cassada,[35] A. Castro,[30] D. Cauz,[40] A. Cerri,[32] A. W. Chan,[1] P. S. Chang,[1] P. T. Chang,[1] J. Chapman,[24] C. Chen,[31] Y. C. Chen,[1] M. -T. Cheng,[1] M. Chertok,[38] G. Chiarelli,[32] I. Chirikov-Zorin,[8] G. Chlachidze,[8] F. Chlebana,[10] L. Christofek,[16] M. L. Chu,[1] Y. S. Chung,[35] C. I. Ciobanu,[27] A. G. Clark,[13] A. Connolly,[21] J. Conway,[37] J. Cooper,[10] M. Cordelli,[12] J. Cranshaw,[39] D. Cronin-Hennessy,[9] R. Cropp,[23] R. Culbertson,[7] D. Dagenhart,[42] F. DeJongh,[10] S. Dell'Agnello,[12] M. Dell'Orso,[32] R. Demina,[10] L. Demortier,[36] M. Deninno,[3] P. F. Derwent,[10] T. Devlin,[37] J. R. Dittmann,[10] S. Donati,[32] J. Done,[38] T. Dorigo,[14] N. Eddy,[16] K. Einsweiler,[21] J. E. Elias,[10] E. Engels, Jr.,[33] W. Erdmann,[10] D. Errede,[16] S. Errede,[16] Q. Fan,[35] R. G. Feild,[45] C. Ferretti,[32] R. D. Field,[11] I. Fiori,[3] B. Flaugher,[10] G. W. Foster,[10] M. Franklin,[14] J. Freeman,[10] J. Friedman,[22] Y. Fukui,[20] I. Furic,[22] S. Galeotti,[32] M. Gallinaro,[36] T. Gao,[31] M. Garcia-Sciveres,[21] A. F. Garfinkel,[34] P. Gatti,[30] C. Gay,[45] S. Geer,[10] D. W. Gerdes,[24] P. Giannetti,[32] P. Giromini,[12] V. Glagolev,[8] M. Gold,[26] J. Goldstein,[10] A. Gordon,[14] A. T. Goshaw,[9] Y. Gotra,[33] K. Goulianos,[36] C. Green,[34] L. Groer,[37] C. Grosso-Pilcher,[7] M. Guenther,[34] G. Guillian,[24] J. Guimaraes da Costa,[14] R. S. Guo,[1] R. M. Haas,[11] C. Haber,[21] E. Hafen,[22] S. R. Hahn,[10] C. Hall,[14] T. Handa,[15] R. Handler,[44] W. Hao,[39] F. Happacher,[12] K. Hara,[41] A. D. Hardman,[34] R. M. Harris,[10] F. Hartmann,[18] K. Hatakeyama,[36] J. Hauser,[5] J. Heinrich,[31] A. Heiss,[18] M. Herndon,[17] B. Hinrichsen,[23] K. D. Hoffman,[34] C. Holck,[31] R. Hollebeek,[31] L. Holloway,[16] R. Hughes,[27] J. Huston,[25] J. Huth,[14] H. Ikeda,[41] J. Incandela,[10] G. Introzzi,[32] J. Iwai,[43] Y. Iwata,[15] E. James,[24] H. Jensen,[10] M. Jones,[31] U. Joshi,[10] H. Kambara,[13] T. Kamon,[38] T. Kaneko,[41] K. Karr,[42] H. Kasha,[45] Y. Kato,[28] T. A. Keaffaber,[34] K. Kelley,[22] M. Kelly,[24] R. D. Kennedy,[10] R. Kephart,[10] D. Khazins,[9] T. Kikuchi,[41] B. Kilminster,[35] M. Kirby,[9] M. Kirk,[4] B. J. Kim,[19] D. H. Kim,[19] H. S. Kim,[16] M. J. Kim,[19] S. H. Kim,[41] Y. K. Kim,[21] L. Kirsch,[4] S. Klimenko,[11] P. Koehn,[27] A. Köngeter,[18] K. Kondo,[43] J. Konigsberg,[11] K. Kordas,[23] A. Korn,[22] A. Korytov,[11] E. Kovacs,[2] J. Kroll,[31] M. Kruse,[35] S. E. Kuhlmann,[2] K. Kurino,[15] T. Kuwabara,[41] A. T. Laasanen,[34] N. Lai,[7] S. Lami,[36] S. Lammel,[10] J. I. Lamoureux,[4] M. Lancaster,[21] G. Latino,[32] T. LeCompte,[2] A. M. Lee IV,[9] K. Lee,[39] S. Leone,[32] J. D. Lewis,[10] M. Lindgren,[5] T. M. Liss,[16] J. B. Liu,[35] Y. C. Liu,[1] N. Lockyer,[31] J. Loken,[29] M. Loreti,[30] D. Lucchesi,[30] P. Lukens,[10] S. Lusin,[44] L. Lyons,[29] J. Lys,[21] R. Madrak,[14] K. Maeshima,[10] P. Maksimovic,[14] L. Malferrari,[3] M. Mangano,[32] M. Mariotti,[30] G. Martignon,[30] A. Martin,[45] J. A. J. Matthews,[26] J. Mayer,[23] P. Mazzanti,[3] K. S. McFarland,[35] P. McIntyre,[38] E. McKigney,[31] M. Menguzzato,[30] A. Menzione,[32] C. Mesropian,[36] A. Meyer,[7] T. Miao,[10] R. Miller,[25] J. S. Miller,[24] H. Minato,[41] S. Miscetti,[12] M. Mishina,[20] G. Mitselmakher,[11] N. Moggi,[3] E. Moore,[26] R. Moore,[24] Y. Morita,[20] M. Mulhearn,[22] A. Mukherjee,[10] T. Muller,[18] A. Munar,[32] P. Murat,[10] S. Murgia,[25] M. Musy,[40] J. Nachtman,[5] S. Nahn,[45] H. Nakada,[41] T. Nakaya,[7] I. Nakano,[15] C. Nelson,[10] D. Neuberger,[18] C. Newman-Holmes,[10] C.-Y. P. Ngan,[22] P. Nicolaidi,[40] H. Niu,[4] L. Nodulman,[2] A. Nomerotski,[11] S. H. Oh,[9] T. Ohmoto,[15] T. Ohsugi,[15] R. Oishi,[41] T. Okusawa,[28] J. Olsen,[44] W. Orejudos,[21] C. Pagliarone,[32] F. Palmonari,[32] R. Paoletti,[32] V. Papadimitriou,[39] S. P. Pappas,[45] D. Partos,[4] J. Patrick,[10] G. Pauletta,[40] M. Paulini,[21] C. Paus,[22] L. Pescara,[30] T. J. Phillips,[9] G. Piacentino,[32] K. T. Pitts,[16] R. Plunkett,[10] A. Pompos,[34] L. Pondrom,[44] G. Pope,[33] M. Popovic,[23] F. Prokoshin,[8] J. Proudfoot,[2] F. Ptohos,[12] O. Pukhov,[8] G. Punzi,[32] K. Ragan,[23] A. Rakitine,[22] D. Reher,[21] A. Reichold,[29] W. Riegler,[14] A. Ribon,[30] F. Rimondi,[3] L. Ristori,[32] W. J. Robertson,[9] A. Robinson,[23] T. Rodrigo,[6] S. Rolli,[42] L. Rosenson,[22] R. Roser,[10] R. Rossin,[30] A. Safonov,[36] W. K. Sakumoto,[35] D. Saltzberg,[5] A. Sansoni,[12] L. Santi,[40] H. Sato,[41] P. Savard,[23] P. Schlabach,[10] E. E. Schmidt,[10] M. P. Schmidt,[45] M. Schmitt,[14] L. Scodellaro,[30] A. Scott,[5] A. Scribano,[32] S. Segler,[10] S. Seidel,[26] Y. Seiya,[41] A. Semenov,[8] F. Semeria,[3] T. Shah,[22] M. D. Shapiro,[21] P. F. Shepard,[33] T. Shibayama,[41] M. Shimojima,[41] M. Shochet,[7] J. Siegrist,[21] G. Signorelli,[32] A. Sill,[39] P. Sinervo,[23] P. Singh,[16] A. J. Slaughter,[45] K. Sliwa,[42] C. Smith,[17] F. D. Snider,[10] A. Solodsky,[36] J. Spalding,[10] T. Speer,[13] P. Sphicas,[22] F. Spinella,[32] M. Spiropulu,[14] L. Spiegel,[10] J. Steele,[44] A. Stefanini,[32] J. Strologas,[16] F. Strumia, [13] D. Stuart,[10] K. Sumorok,[22] T. Suzuki,[41] T. Takano,[28] R. Takashima,[15] K. Takikawa,[41] P. Tamburello,[9] M. Tanaka,[41] B. Tannenbaum,[5] W. Taylor,[23] M. Tecchio,[24] P. K. Teng,[1] K. Terashi,[36] S. Tether,[22] D. Theriot,[10] R. Thurman-Keup,[2] P. Tipton,[35]

S. Tkaczyk,[10] K. Tollefson,[35] A. Tollestrup,[10] H. Toyoda,[28] W. Trischuk,[23] J. F. de Troconiz,[14] J. Tseng,[22] N. Turini,[32] F. Ukegawa,[41] T. Vaiciulis,[35] J. Valls,[37] S. Vejcik III,[10] G. Velev,[10] R. Vidal,[10] R. Vilar,[6] I. Volobouev,[21] D. Vucinic,[22] R. G. Wagner,[2] R. L. Wagner,[10] J. Wahl,[7] N. B. Wallace,[37] A. M. Walsh,[37] C. Wang,[9] C. H. Wang,[1] M. J. Wang,[1] T. Watanabe,[41] D. Waters,[29] T. Watts,[37] R. Webb,[38] H. Wenzel,[18] W. C. Wester III,[10] A. B. Wicklund,[2] E. Wicklund,[10] H. H. Williams,[31] P. Wilson,[10] B. L. Winer,[27] D. Winn,[24] S. Wolbers,[10] D. Wolinski,[24] J. Wolinski,[25] S. Wolinski,[24] S. Worm,[26] X. Wu,[13] J. Wyss,[32] A. Yagil,[10] W. Yao,[21] G. P. Yeh,[10] P. Yeh,[1] J. Yoh,[10] C. Yosef,[25] T. Yoshida,[28] I. Yu,[19] S. Yu,[31] Z. Yu,[45] A. Zanetti,[40] F. Zetti,[21] and S. Zucchelli[3]

(CDF Collaboration)

[1] *Institute of Physics, Academia Sinica, Taipei, Taiwan 11529, Republic of China*
[2] *Argonne National Laboratory, Argonne, Illinois 60439*
[3] *Istituto Nazionale di Fisica Nucleare, University of Bologna, I-40127 Bologna, Italy*
[4] *Brandeis University, Waltham, Massachusetts 02254*
[5] *University of California at Los Angeles, Los Angeles, California 90024*
[6] *Instituto de Fisica de Cantabria, CSIC-University of Cantabria, 39005 Santander, Spain*
[7] *Enrico Fermi Institute, University of Chicago, Chicago, Illinois 60637*
[8] *Joint Institute for Nuclear Research, RU-141980 Dubna, Russia*
[9] *Duke University, Durham, North Carolina 27708*
[10] *Fermi National Accelerator Laboratory, Batavia, Illinois 60510*
[11] *University of Florida, Gainesville, Florida 32611*
[12] *Laboratori Nazionali di Frascati, Istituto Nazionale di Fisica Nucleare, I-00044 Frascati, Italy*
[13] *University of Geneva, CH-1211 Geneva 4, Switzerland*
[14] *Harvard University, Cambridge, Massachusetts 02138*
[15] *Hiroshima University, Higashi-Hiroshima 724, Japan*
[16] *University of Illinois, Urbana, Illinois 61801*
[17] *The Johns Hopkins University, Baltimore, Maryland 21218*
[18] *Institut für Experimentelle Kernphysik, Universität Karlsruhe, 76128 Karlsruhe, Germany*
[19] *Korean Hadron Collider Laboratory: Kyungpook National University, Taegu 702-701; Seoul National University, Seoul 151-742; and SungKyunKwan University, Suwon 440-746; Korea*
[20] *High Energy Accelerator Research Organization (KEK), Tsukuba, Ibaraki 305, Japan*
[21] *Ernest Orlando Lawrence Berkeley National Laboratory, Berkeley, California 94720*
[22] *Massachusetts Institute of Technology, Cambridge, Massachusetts 02139*
[23] *Institute of Particle Physics: McGill University, Montreal H3A 2T8; and University of Toronto, Toronto M5S 1A7; Canada*
[24] *University of Michigan, Ann Arbor, Michigan 48109*
[25] *Michigan State University, East Lansing, Michigan 48824*
[26] *University of New Mexico, Albuquerque, New Mexico 87131*
[27] *The Ohio State University, Columbus, Ohio 43210*
[28] *Osaka City University, Osaka 588, Japan*
[29] *University of Oxford, Oxford OX1 3RH, United Kingdom*
[30] *Universita di Padova, Istituto Nazionale di Fisica Nucleare, Sezione di Padova, I-35131 Padova, Italy*
[31] *University of Pennsylvania, Philadelphia, Pennsylvania 19104*
[32] *Istituto Nazionale di Fisica Nucleare, University and Scuola Normale Superiore of Pisa, I-56100 Pisa, Italy*
[33] *University of Pittsburgh, Pittsburgh, Pennsylvania 15260*
[34] *Purdue University, West Lafayette, Indiana 47907*
[35] *University of Rochester, Rochester, New York 14627*
[36] *Rockefeller University, New York, New York 10021*
[37] *Rutgers University, Piscataway, New Jersey 08855*
[38] *Texas A&M University, College Station, Texas 77843*
[39] *Texas Tech University, Lubbock, Texas 79409*
[40] *Istituto Nazionale di Fisica Nucleare, University of Trieste/ Udine, Italy*
[41] *University of Tsukuba, Tsukuba, Ibaraki 305, Japan*
[42] *Tufts University, Medford, Massachusetts 02155*
[43] *Waseda University, Tokyo 169, Japan*
[44] *University of Wisconsin, Madison, Wisconsin 53706*
[45] *Yale University, New Haven, Connecticut 06520*

We report on the first measurement of the rapidity distribution $d\sigma/dy$ over nearly the entire kinematic region of rapidity for e^+e^- pairs in the Z-boson region of $66 < M_{ee} < 116$ GeV/c^2 and at higher mass $M_{ee} > 116$ GeV/c^2. The data sample consists of 108 pb^{-1} of $p\bar{p}$ collisions at

$\sqrt{s} = 1.8$ TeV taken by the Collider Detector at Fermilab during 1992–1995. The total cross section in the Z-boson region is measured to be 252 ± 11 pb. The measured total cross section and $d\sigma/dy$ are compared with quantum chromodynamics calculations in leading and higher orders.

PACS numbers: 13.85.Qk, 12.38.Qk

Most measurements at high energy proton-antiproton colliders are performed in the central rapidity production region, $|y| < 1$. A model dependent extrapolation for $|y| > 1$ is needed to extract the total cross section for hard processes such as top quark production or W and Z boson production. This extrapolation is made using Monte Carlo programs (e.g. PYTHIA [1]), which incorporate quantum chromodynamics (QCD) calculations in leading order (LO) or next to leading order (NLO). A previous measurement of the rapidity distribution, $d\sigma/dy$, for dimuon pairs in the Z-bosons mass region was limited to $|y| < 1$ [2]. In this communication, we present the first measurement of $d\sigma/dy$ for e^+e^- pairs in the Z-boson mass and high mass region over nearly the entire kinematic region of rapidity. At the Tevatron $p\bar{p}$ collider, the kinematic limit at the Z-boson mass is $|y| = 3.0$, while we measure $|y|$ up to 2.8. The $d\sigma/dy$ distributions are compared to the predictions of QCD in LO and NLO. This measurement is also relevant for precision W boson mass measurements at hadron colliders, where W's are reconstructed using $e\nu$ and $\mu\nu$ pairs from the Drell-Yan process.

In hadron-hadron collisions at high energies, massive e^+e^- pairs are produced via the Drell-Yan [3] process. In the standard model, quark-antiquark annihilation form an intermediate γ^* or Z (γ^*/Z) vector boson, which then decays into an e^+e^- pair. In LO, the momentum fraction x_1 (x_2) of the partons in the proton (antiproton) are related to the rapidity [4], y, of the boson via the equation $x_{1,2} = (M/\sqrt{s})e^{\pm y}$. Here s is the center of mass energy, and M is the mass of the dilepton pair. Therefore, dilepton pairs which are produced at large rapidity originate from events in which one parton is at large x and another parton is at very small x. Since the quark distributions for x up to 0.9 are well constrained by the deep-inelastic lepton scattering experiments [5], comparisons of data and theory for $d\sigma/dy$, and the total cross sections provide a test of the theory, e.g. missing NNLO [6,7] or power correction [8] terms.

The e^+e^- pairs are from 108 pb^{-1} of $p\bar{p}$ collisions at $\sqrt{s} = 1.8$ TeV taken by the Collider Detector at Fermilab [4] (CDF) during 1992–1993 (18.7 ± 0.7 pb^{-1}) and 1994–1995 (89.1 ± 3.7 pb^{-1}). CDF is a solenoidal magnetic spectrometer surrounded by projective-tower-geometry calorimeters and outer muon detectors. Only detector components used in this measurement are described here. Charged particle momenta and directions are measured by the spectrometer, which consists of a 1.4 T axial magnetic field, an 84-layer cylindrical drift chamber (CTC), an inner vertex tracking chamber (VTX), and a silicon vertex detector (SVX). The polar coverage of the CTC tracking is $|\eta| < 1.2$. The $p\bar{p}$ collision point along the beam line ($Z_{\rm vertex}$) is determined using tracks in the VTX. The energies and directions [4] of electrons, photons, and jets are measured by three separate calorimeters covering three regions: central ($|\eta| < 1.1$), end plug ($1.1 < |\eta| < 2.4$), and forward ($2.2 < |\eta| < 4.2$). Each region has an electromagnetic (EM) and hadronic (HAD) calorimeter.

In a previous letter, we presented $d\sigma/dP_{\rm T}$ of Z boson [9]. This analysis is an extension of the $d\sigma/dP_{\rm T}$ measurement. The $d\sigma/dP_{\rm T}$ analysis has three categories of e^+e^- pairs: central-central (CC), central-end plug (CP), and central-forward (CF). This analysis extends the sample to the forward rapidity region by including plug-plug (PP) and plug-forward (PF) events. The inclusion of these events increases the event sample by 20% and allows for measurement of Z bosons with $|y|$ up to 2.8. An improvement in this analysis is the additional VTX tracking requirements for plug and forward electrons. The VTX covers the entire rapidity range in this study, and plays an important role in removing background in the high η region which is not covered by the CTC.

The sample of e^+e^- events was collected by a three-level online trigger that required an electron in either the central or the plug calorimeter. The offline analysis selects events with two or more electron candidates. Since the electrons from the Drell-Yan process are typically isolated, both electrons are required to be isolated from any other activity in the calorimeters. Electrons in the central, end plug, and forward regions are required to be within the fiducial area of the calorimeters and have a minimum $E_{\rm T}$ of 22, 20, and 15 GeV, respectively. To improve the purity of the sample, electron identification cuts are applied [9]. For CC, CP, and CF events, the central electron (or one of them if there are two) is required to pass strict criteria. The criteria on the other electron are looser. A central electron must have a CTC track that extrapolates to the electron's shower clusters in the EM calorimeter. These clusters must have EM-like transverse shower profiles. The track momentum and the EM shower energy must be consistent with one another. The track is also used to determine the position and direction of the central electron. The fraction of energy in the HAD calorimeter towers behind the EM shower is required to be consistent with that expected for an EM shower ($E_{\rm HAD}/E_{\rm EM}$). The plug electrons must also have an EM-like transverse shower profile. The end plug and forward electrons are required to pass the $E_{\rm HAD}/E_{\rm EM}$ requirement and to have a track in the VTX which originates from the same vertex as the other electron and points to the position of the electromagnetic cluster in the calorimeter. The ratio of found to expected hits in the VTX is required to be greater than 70% and 50% for plug and forward electrons, respectively. The VTX tracking efficiency is $(97.8 \pm 0.3)\%$ for plug electrons and $(97.0 \pm 0.9)\%$ for forward electrons. This requirement on plug and forward electrons reduce the background rates from 11% to 2% for PP events, and from 22% to 4% for PF events.

The data sample is divided into two mass bins: the Z region ($66 < M_{ee} < 116$ GeV$/c^2$) and the high mass region ($M_{ee} > 116$ GeV$/c^2$). After all cuts, the numbers of CC, CP, CF, PP, and PF events in the Z mass region are 2894, 3811, 621, 1236, and 589, respectively. The backgrounds are low and are estimated using the data.

The backgrounds in the CP, CF, PP, and PF topologies are dominated by jets and are 28 ± 5, 13 ± 3, 24 ± 2, and 23 ± 3 events, respectively. Because of the CTC tracking requirement, the jet background for the CC sample is negligible. The CC background is mainly from e^+e^- pairs from W^+W^-, $\tau^+\tau^-$, $c\bar{c}$, $b\bar{b}$, and $t\bar{t}$ sources. This background, estimated using $e^{\pm}\mu^{\mp}$ pairs [10], is 3 ± 2 events. In the high mass bin, the numbers of CC, CP, CF, PP, and PF events are 61, 59, 9, 18, and 5, respectively. The mean mass of the high mass bin is 152.6 GeV/c^2.

The acceptance for Drell-Yan e^+e^- pairs is obtained using the Monte Carlo event generator, PYTHIA [1], and CDF detector simulation programs. PYTHIA generates the LO QCD interaction ($q + \bar{q} \rightarrow \gamma^*/Z$), simulates initial state QCD radiation via its parton shower algorithms, and generates the decay, $\gamma^*/Z \rightarrow e^+e^-$. To approximate higher order QCD corrections to the LO mass distribution, a "K-factor" [11] is used as an event weight: $K(M^2) = 1 + \frac{4}{3}(1 + \frac{4}{3}\pi^2)\alpha_s(M^2)/2\pi$, where α_s is the two loop QCD coupling. This factor improves the agreement between the NLO and LO mass spectra. (For $M > 50$ GeV/c^2, $1.25 < K < 1.36$.) The CTEQ3L [12] PDFs are used in the acceptance calculations. Final state QED radiation [13] from the $\gamma^*/Z \rightarrow e^+e^-$ vertex is added by the PHOTOS [14] Monte Carlo program. Generated events are processed by CDF detector simulation programs and are reconstructed as data. The calorimetry energy scales and resolutions used in the detector simulation are extracted from the data, as are the cut efficiencies and corresponding errors. Simulated events are accepted if after the reconstruction they pass the e^+e^- pair mass, the detector fiducial, and kinematic (E_T) cuts.

In the $d\sigma/dy$ measurement, various samples are combined and binned in y. The $d\sigma/dy$ is calculated with

$$\frac{d\sigma}{dy} = \frac{\Delta N}{C\ \Delta y\ \sum_r \mathcal{L}_r\ \epsilon A_r}.$$

The ΔN is the background-subtracted event count in a y bin, C is a bin centering correction, Δy is the bin width, the sum r is over the 1992–1993 and 1994–1995 runs, $\mathcal{L}_r$ is the integrated luminosity, and ϵA_r is the run's combined event selection efficiency and acceptance. The backgrounds subtracted from the event count are predicted using the data and background samples. The factor C corrects the average value of the cross section in the bin to its bin center value. Acceptances are calculated separately for CC, CP, CF, PP, and PF pairs. They are combined with the corresponding event selection efficiencies to give ϵA_r. Figure 1 shows the ϵA_r for events in the Z region as a function of y for the CC sample, the CC+CP+CF sample, and the CC+CP+CF+PP+PF sample, respectively. It indicates that the PP+PF events extend the acceptance of the y measurement to $|y| = 2.8$. We significantly increase our statistics by extending the acceptance beyond $y > 1.2$. The $d\sigma/dy$ of e^+e^- events in the Z mass region is shown in Table I.

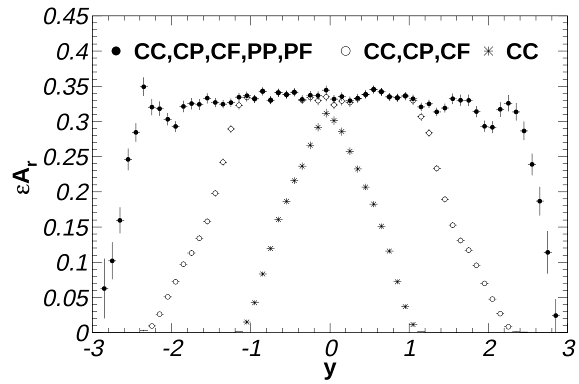

FIG. 1. The efficiency times acceptance for e^+e^- pairs in the Z boson mass region: (a) for the CC sample (asterisks), (b) for the CC+CP+CF sample (open circles), and (c) for the CC+CP+CF+PP+PF sample (solid circles).

The systematic errors considered are from variations in the background estimates using different methods, the background in the efficiency sample, the uncertainty in energy resolution of the calorimeter, the choice of PDFs, and the distribution of Z $P_{\rm T}$ used in the Monte Carlo event generator. The systematic error from the calorimeter resolution is 0.2% in the low y region and increases to 0.7% at $|y| > 2.5$. The systematic error from variations in the Z $P_{\rm T}$ is 0.5% at $|y| = 0$ and is 2.0% at $|y| = 2.8$. The systematic error from the choice of PDFs is less than 1% in $|y| < 2.0$ and increases to 2% at $|y| = 2.8$. For the total cross section measurement, the combined systematic error is 0.6% (excluding the luminosity uncertainty). The $p\bar{p}$ collision luminosity is derived with CDF's beam-beam cross section, $\sigma_{\rm BBC} = 51.15 \pm 1.60$ mb [15,16]. The luminosity error of 3.9% contains the $\sigma_{\rm BBC}$ error and uncertainties specific to running conditions.

Figures 2(a) and 2(b) compare the measured $d\sigma/dy$'s to theoretical predictions in the Z mass and high mass regions, respectively. The top horizontal axes on these figures are the corresponding values of the x_1 and x_2 as a function of y. The predictions are LO calculations with CTEQ5L [17] PDFs and NLO [18] calculations with MRST99 [19] and CTEQ5M-1 [17] PDFs. The predictions in Figure 2(a) have been normalized by a factor "F", the ratio of measured total cross section to the prediction (F=1.51, 1.14, and 1.13 for the CTEQ5L, MRST99 and CTEQ5M-1 PDFs, respectively). The predictions in Figure 2(b) are normalized to the data using the factor F from the Z mass region. We compare the data to the theory using statistical errors only. As the χ^2 values listed in Figure 2(a) indicate, the LO calculation using recent LO PDFs does not fit the shape as well as the NLO calculation with the most recent NLO PDFs.

Model independent measurements of the total production cross sections for e^+e^- pairs are extracted by integrating the measured values of $d\sigma/dy$. Because there are no data for $|y| > 2.8$, we use a NLO calculation with the CTEQ5M-1 PDFs to estimate γ^*/Z production in that region. The cross section in the region of $|y| > 2.8$ is about 0.02% of the predicted total cross section. The extracted cross section in the Z mass region is 252.1 ± 3.9 (stat.) $\pm$ 1.6 (syst.) $\pm$ 9.8 (lum.) pb. The corresponding $\sigma(p\bar{p} \to Z) \cdot Br(Z \to ee)$ is $253 \pm 4(\text{stat.} + \text{syst.}) \pm 10(\text{lum.})$ pb. This measurement is in agreement with our previous measurements in the di-electron [9] ($248 \pm 5(\text{stat.} + \text{syst.}) \pm 10(\text{lum.})$ pb, using only the CC+CP+CF e^+e^- sample), and dimuon [2] ($237 \pm 9(\text{stat.} + \text{syst.}) \pm 9(\text{lum.})$ pb using a CC sample) channels. These previous measurements use a QCD model to correct for the missing events at high rapidity. The combined e^+e^- and $\mu^+\mu^-$ cross section is 250 ± 4(stat.+syst.)$\pm$10 pb. Since the $p\bar{p}$ inelastic cross section used by CDF in luminosity calculations differs from DØ's by +5.9% [16], measured cross sections must be renormalized before comparisons to other experiments. The DØ measurement [20] of 221 ± 11 pb when renormalized to the CDF luminosity measurement is 234 ± 12 pb.

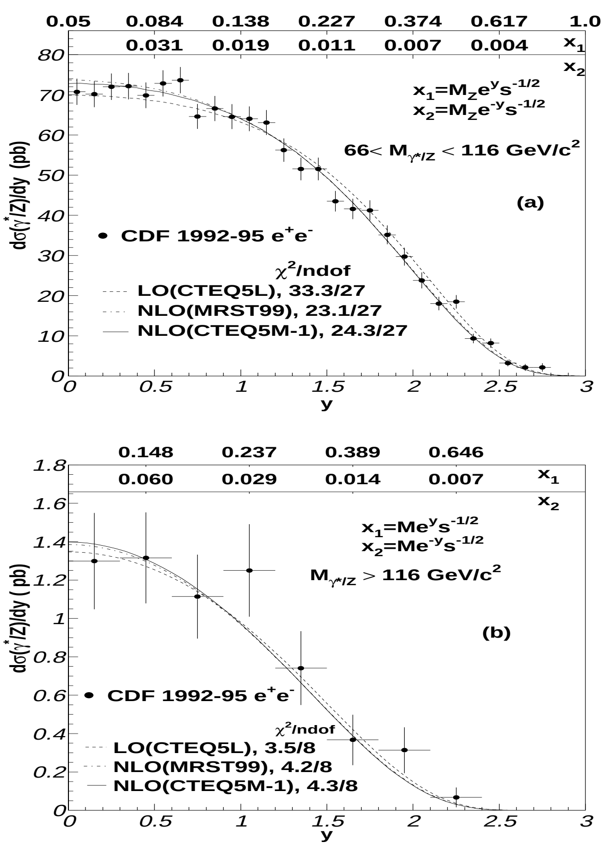

FIG. 2. $d\sigma/dy$ distribution of e^+e^- pairs: (a) in the Z boson mass ($66 < M_{ee} < 116$ GeV/c^2) region. (b) in the high mass ($M_{ee} > 116$ GeV/c^2) region. The M used to obtain x_1 and x_2 in (b) is the mean mass over the bin. The error bars on the data include statistical errors only. The theoretical predictions have been normalized to the data in the Z boson mass region.

The total cross section measurements can also be compared to QCD calculations. Fixed order QCD calculations have uncertainties from PDF measurements and corrections from higher orders of perturbation theory, i.e., the K-factor. The NLO-to-LO total cross section correction is significant: $K \sim 1.4$. In contrast, the NLO total cross section is lower than NNLO [6] prediction by only 2.3%. The NNLO prediction with the latest NLO MRST99 PDFs is 227$\pm$9 pb, where the 4% error is mostly from uncertainties [19] in the NLO PDFs. Although a full set of NNLO PDFs is not available, recent estimates [7] of NNLO PDFs indicate that the NNLO PDFs will increase the theoretical cross sections by 5%. Given these uncertainties, the theoretical expectation is consistent with the Z cross section measurements.

The measurement of the Drell-Yan total cross section in the high mass region is 4.0 ± 0.4 (stat. + syst.) $\pm$ 0.2 (lum.) pb. The corresponding prediction of the total cross section from the NNLO QCD theory using MRST99 PDFs is 3.3 pb.

In summary, the rapidity distributions of e^+e^- pairs in the Z boson mass and high mass region have been measured for the first time over nearly the entire kinematic region. This measurement uses a new tracking technique in the high rapidity region to reduce the background and uncertainties associated with it. In addition, unlike the previous measurement of the total cross section, this measurement is model independent.

The vital contributions of the Fermilab staff and the technical staffs of the participating institutions are gratefully acknowledged. This work is supported by the U.S. Department of Energy and National Science Foundation; the Natural Sciences and Engineering Research Council of Canada; the Istituto Nazionale di Fisica Nucleare of Italy; the Ministry of Education, Science and Culture of Japan; the National Science Council of the Republic of China; the A.P. Sloan Foundation, and the Swiss National Science Foundation.

---

[1] T. Sjöstrand, Comput. Phys. Commun. **82**, 74 (1994). The default PYTHIA 6.104 is used except `MSTJ(41)=1`, `MSTP(91)=2`, and `PARP(92,93)=1.25,10.0` GeV.

[2] F. Abe *et al.*, Phys. Rev. D **59**, 052002 (1999).

[3] S.D. Drell and T.-M. Yan, Phys. Rev. Lett. **25**, 316 (1970).

[4] F. Abe *et al.*, Nucl. Instrum. Methods Phys. Res. Sect. A **271**, 387 (1988). CDF coordinates are in (θ, ϕ, z), where θ is the polar angle relative to the proton beam (the $+z$ axis), and ϕ the azimuth. The pseudorapidity is $\eta = -\ln\tan(\theta/2)$. Here $P_{\rm T} = P\sin\theta$, $y = \frac{1}{2}ln\frac{P+P_z}{P-P_z}$, P and P_z are the magnitude and z component of a particle's momentum, and $E_{\rm T} = E\sin\theta$, where E is the energy measured in the calorimeter.

[5] U. K. Yang and A. Bodek, Phys. Rev. Lett. **82**, 2467 (1999).
[6] $\overline{\text{MS}}$: R. Hamberg, W.L. van Neerven, and T. Matsuura, Nucl. Phys. B **359**, 343 (1991). DIS :W. L. Van Neerven and E. B. Zijlstra, Nucl. Phys. B **382**, 11 (1992).
[7] U.K. Yang and A. Bodek, Euro. Phys. Jour. C **13**, 241 (2000); W.L. van Neerven and A. Vogt, Nucl. Phys. B **568**, 263 (2000), hep-ph/9907472.
[8] M. Dasgupta, J. High Energy Phys. 12(1999) 008.
[9] T. Affolder *et al.*, Phys. Rev. Lett. **84**, 845 (2000).
[10] The CDF top-quark high-$P_{\rm T}$ dilepton selection (F. Abe *et al.*, Phys. Rev. D **50**, 2966 (1994)) is used, but with both leptons isolated and no jet cuts.
[11] G. Altarelli, R. E. Ellis, and G. Martinelli, Nucl. Phys. B **157**, 461 (1979).
[12] H. L. Lai *et al.*, Phys. Rev. D **51**, 4763 (1995). The old PDF CTEQ3L is used in the acceptance calculation since it happens to describe the shape of the y distribution well (χ^2 = 21.2/ndof, F=1.55).
[13] U. Baur, S. Keller, and W. K. Sakumoto, Phys. Rev. D **57**, 199 (1998).
[14] E. Barberio and Z. Was, Comput. Phys. Commun. **79**, 291 (1994); E. Barberio, B. van Eijk, and Z. Was, *ibid.* **66**, 115 (1991).
[15] F. Abe *et al.*, Phys. Rev. Lett. **76**, 3070 (1996).
[16] D. Cronin-Hennessy *et al.*, Nucl. Instrum. Methods Phys. Res., Sect. A **443/1**, 37-50 (2000)
[17] H. L. Lai *et al.*, Eur. Phys. J. C12, 375 (2000)
[18] P. J. Rijken and W. L. van Neerven, Phys. Rev. D. **51**, 44 (1995)
[19] A.D. Martin *et al.*, Eur. Phys. J. C14,133 (2000). Note that the QCD evolution code used by the MRST99 and CTEQ5M-1 PDFs are now in agreement with each other.
[20] B. Abbott *et al.*, Phys. Rev. D. **61**, 072001 (2000).

TABLE I. $d\sigma/dy$ distribution of e^+e^- events in the mass range $66 < M_{ee} < 116$ GeV/c^2. The first and second errors are statistical and systematic, respectively. The 3.9% luminosity error is not included. Here y is the bin center value.

y	$d\sigma/dy$ [pb]	y	$d\sigma/dy$ [pb]
0.05	$70.78 \pm 3.27 \pm 0.37$	1.45	$51.56 \pm 2.82 \pm 0.45$
0.15	$70.19 \pm 3.26 \pm 0.37$	1.55	$43.51 \pm 2.56 \pm 0.39$
0.25	$72.03 \pm 3.30 \pm 0.41$	1.65	$41.62 \pm 2.54 \pm 0.45$
0.35	$72.18 \pm 3.30 \pm 0.45$	1.75	$41.24 \pm 2.53 \pm 0.46$
0.45	$69.90 \pm 3.20 \pm 0.50$	1.85	$35.15 \pm 2.35 \pm 0.40$
0.55	$72.86 \pm 3.25 \pm 0.59$	1.95	$29.72 \pm 2.23 \pm 0.36$
0.65	$73.68 \pm 3.27 \pm 0.64$	2.05	$23.80 \pm 1.98 \pm 0.33$
0.75	$64.64 \pm 3.09 \pm 0.58$	2.15	$18.04 \pm 1.68 \pm 0.29$
0.85	$66.59 \pm 3.13 \pm 0.63$	2.25	$18.47 \pm 1.70 \pm 0.33$
0.95	$64.59 \pm 3.10 \pm 0.67$	2.35	$9.35 \pm 1.17 \pm 0.19$
1.05	$64.04 \pm 3.09 \pm 0.70$	2.45	$8.20 \pm 1.17 \pm 0.19$
1.15	$63.11 \pm 3.10 \pm 0.67$	2.55	$3.24 \pm 0.80 \pm 0.08$
1.25	$56.26 \pm 2.92 \pm 0.55$	2.65	$2.15 \pm 0.85 \pm 0.06$
1.35	$51.57 \pm 2.82 \pm 0.45$	2.75	$2.14 \pm 1.02 \pm 0.06$